and the 36B4 reactions to facilitate ATLR calculation. Ct values were converted to ng values according to the standard curves. ng values of the telomere (T) reaction were divided by the ng values of the 36B4 (S) reaction to yield the ATLR. The primer sequences for the telomere portion were as follows: 5'-CGGTTTGTTTGGGTTTGGGTTTGGGTTTGGGTTTGGGTT-3' and 5'-GGCTTGCCTTACCCTTACCCTTACCCTTACCCTTACCCT-3'. The primer sequences for the 36B4 single copy gene portion were as follows: 5'-ACTGGTCTAGGACCCGAGAAG-3' and 5'-TCAATGGTGCCTCTGGAGATT-3'. Cycling conditions for both primer sets (run in the same plate) were: 95°C for 10 min, 30 cycles of 95°C for 15 s, and 55°C for 1 min for annealing and extension.

FlexiVent

Mice were anesthetized, tracheostomized with a 20-gauge Angiocath, and placed on a forced system for measurement of lung mechanics with the use of a FlexiVent mouse ventilator (Scireq, Montreal, Canada). According to the protocols established by Scireq [7], a standard ventilation history for each mouse was first obtained with three total lung capacity (TLC) maneuvers to determine mean displaced volume (Vend), Vend relative to weight, and mean delivered volume. Then, a "snapshot perturbation" maneuver was imposed to measure resistance (R), compliance (C), and elastance (E). Subsequently, a forced oscillation perturbation ("primewave-8") was applied to measure airway resistance (Rn), inertia of the air, tissue damping (resistance) (G), elasticity (H), and tissue hysteresivity (tissue damping [G]/H). Finally, pressure-volume (PV) loops (PVs-V = PV-stepwise-volume regulated; PVr-V = PV-ramp-volume regulated; PVr-P = PV-ramp pressure regulated) were generated to obtain maximal vital (total) lung capacity (A), inspiratory capacity (IC) from zero pressure (B), form of deflating PV loop (K), static compliance (Cst), static elastance (Est), and hysteresis (area between inflating and deflating part of the loop).

For FlexiVent perturbations, a coefficient of determination of 0.95 was the lower limit for accepting a measurement. For each parameter, an average of three measurements was calculated per mouse.

Lung inflation

A 20-gauge Angiocath was sutured into the trachea. The bronchi to the right lung was tied off so that the right lung could be removed for other analysis. The remaining left lung was inflated to 15 cm H_2O with 10% paraformaldehyde (PFA) by attaching the Angiocath to a syringe filled with PFA that was elevated to 15 cm above the bench. This allowed gravity to force PFA into the lung equally in all samples, leading to expansion.

Mean linear intercept calculation

The inflated lungs were paraffin embedded and sectioned at 6 microns. The lung was cut until clear, continuous branching of the bronchi was observed (slicing through the middle of the lung in the xy plane). Lung sections were stained with hematoxylin and eosin (H & E). The whole lung was then imaged at 20x objective using the TissueGnostics (Vienna, Austria) software and microscope located at the Northwestern University Cell Imaging Facility/Nikon Imaging Center (generously supported by NCI CCSG P30 CA060553 awarded to the Robert H. Lurie Comprehensive Cancer Center). The outline of the whole lung is traced, and the automated microscope takes serial 20x images covering the entirety of the traced area.

After imaging, 20 pictures from each lung were randomly selected using a random number generator to undergo mean linear intercept (MLI) quantification with the ImagePro software mentioned above. Each selected section had to be completely occupied by lung tissue and not contain large bronchi, vessels, or other miscellaneous tissue. A blank picture from that same

slide was subtracted off of the selected 20 images for background correction. Using the color picking tools of the software, any area occupied by tissue was highlighted. Next, the overall image was converted into a binary picture and then inverted so that the tissue was colored black and the airspace colored white. A 6x7 grid was then superimposed on top of the black and white lung image. Using the operations tool, a new picture was generated showing where the grid and the lung tissue overlap. The number of intercepts was counted (including adding extra for any place where two of the grid lines intersected each other and tissue, as this would only be counted as one object by the software). MLI was determined by dividing the total length of the grid lines by the total number of intercepts (in this case, 11,541 μm/# intercepts).

Statistical analysis

All results are presented as mean ± SD. Comparisons between 2 groups were tested by an unpaired, 2-tailed Student's *t* test (unless otherwise noted). Results with $P \leq 0.05$ were considered significant.

Results

As with previous studies [1,2,3], we investigated the effects of L-NAME (1 mg/mL) or regular water for 8 weeks in 6–8 week old C57BL/6J mice [8]. We observed that L-NAME-treated mice exhibited a substantial amount of alveolar tissue obliteration resembling emphysema (Fig. 1B) compared to controls that ingested unmodified drinking water (Fig. 1A). Since loss of PAI-1 activity has been shown to be protective against L-NAME-induced pathologies, we evaluated whether genetic deficiency or pharmacologic inhibition of PAI-1 would attenuate L-NAME-induced emphysema. This was accomplished by either administering L-NAME to PAI-1 knockout (PAI-$1^{-/-}$) mice or by co-treating WT mice with L-NAME and the small molecule antagonist TM5441 (described previously in [3]). Compared to animals on L-NAME alone, the L-NAME + TM5441 and the PAI-$1^{-/-}$ + L-NAME mice had substantially less alveolar tissue loss (Fig. 1C and 1D). We quantified the extent of emphysema in these animals by calculating mean linear intercept (MLI) in lung histology sections. As shown in Fig. 1E, animals given L-NAME had a higher MLI compared to WT (72.7 ± 4.0 μm vs. 62.3 ± 5.5 μm, P = 0.0002). However, this increase was partially attenuated by both genetic deficiency (68.5 ± 3.4 μm, P = 0.04 vs. WT + L-NAME) and pharmacologic inhibition (68.7 ± 3.6 μm, P = 0.04 vs. WT + L-NAME) of PAI-1.

We also measured lung functional dynamics using the FlexiVent mouse ventilator. Compliance and elastance were each measured 2 ways using different perturbations. As shown in Fig. 2, we found that animals treated with L-NAME had both a higher compliance (C) and static compliance (Cst) than WT animals (P = 0.002 and P = 0.004, respectively), consistent with the development of emphysema. The same was true for the inverse measurement, as L-NAME-treated animals had lower values for both elastance (E) and static elastance (Est). However, when L-NAME was administered to either PAI-1-deficient animals or mice treated with TM5441, the values for C, Cst, E, and Est were all similar to WT controls, indicating that these animals were protected against emphysema development. These FlexiVent findings are consistent with the interpretation that PAI-1contributes to the development of L-NAME-induced emphysema.

Since there is no precedent in the literature of using chronic L-NAME administration as a model for emphysema, we investigated the mechanism behind alveolar tissue loss in these animals. First, we examined if L-NAME could promote the development of senescence similar to that previously seen in the aorta [3]. After 8 weeks of treatment, telomere length in the lung of L-NAME-treated animals was decreased (P = 0.007 vs. WT), and TM5441 co-treatment prevented this reduction (P = 0.007 vs. WT + L-NAME) (Fig. 3A). However, when the expression levels of the senescence marker $p16^{Ink4a}$ were measured, there was no difference between L-

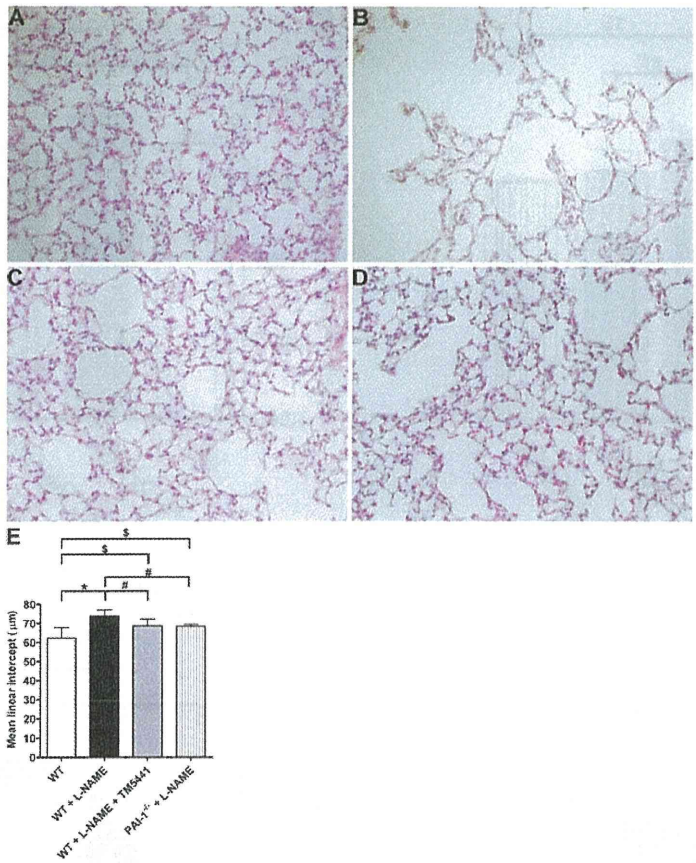

Fig 1. L-NAME treatment causes emphysema. Lung tissue sections from **(A)** WT, **(B)** WT + L-NAME, **(C)** WT + L-NAME + TM5441, and **(D)** PAI-1-/- + L-NAME demonstrate that L-NAME causes significant alveolar destruction and that PAI-1 inhibition is partially protective against this. **(E)** Mean linear intercept quantifications. *P = 0.0002, #P = 0.04, $P = 0.009. Data are mean ± SD. n = 11–13.

doi:10.1371/journal.pone.0116504.g001

NAME-treated and untreated mice. Since emphysema is already established at 8 weeks, we hypothesized that the cells that had expressed $p16^{Ink4a}$ may have been already cleared, leading to the tissue loss characteristic of emphysema. Therefore, we looked at earlier time points in order to identify evidence of senescence prior to the development of emphysema. As shown in Fig. 3B, after one week on L-NAME, $p16^{Ink4a}$ expression was increased in the lung. Notably, there was a detectable difference in $p16^{Ink4a}$ expression between the L-NAME and the L-NAME + TM5441 groups at this early time point (P = 0.02). Although not significant, a similar pattern is also seen when looking at other senescent markers such as p53 (Fig. 3C) and p21 (Fig. 3D). This data indicates that L-NAME triggers cellular senescence relatively rapidly after initiating the treatment. Together with the telomere length results, these findings indicate that L-NAME-induced emphysema may be mediated through cellular senescence.

Discussion

The present study represents the first report of using L-NAME treatment to induce emphysema. However, this work is not the first to examine the role of NOS inhibition in lung disease. Several prior reports have focused on the role of iNOS in emphysema. In general, these studies

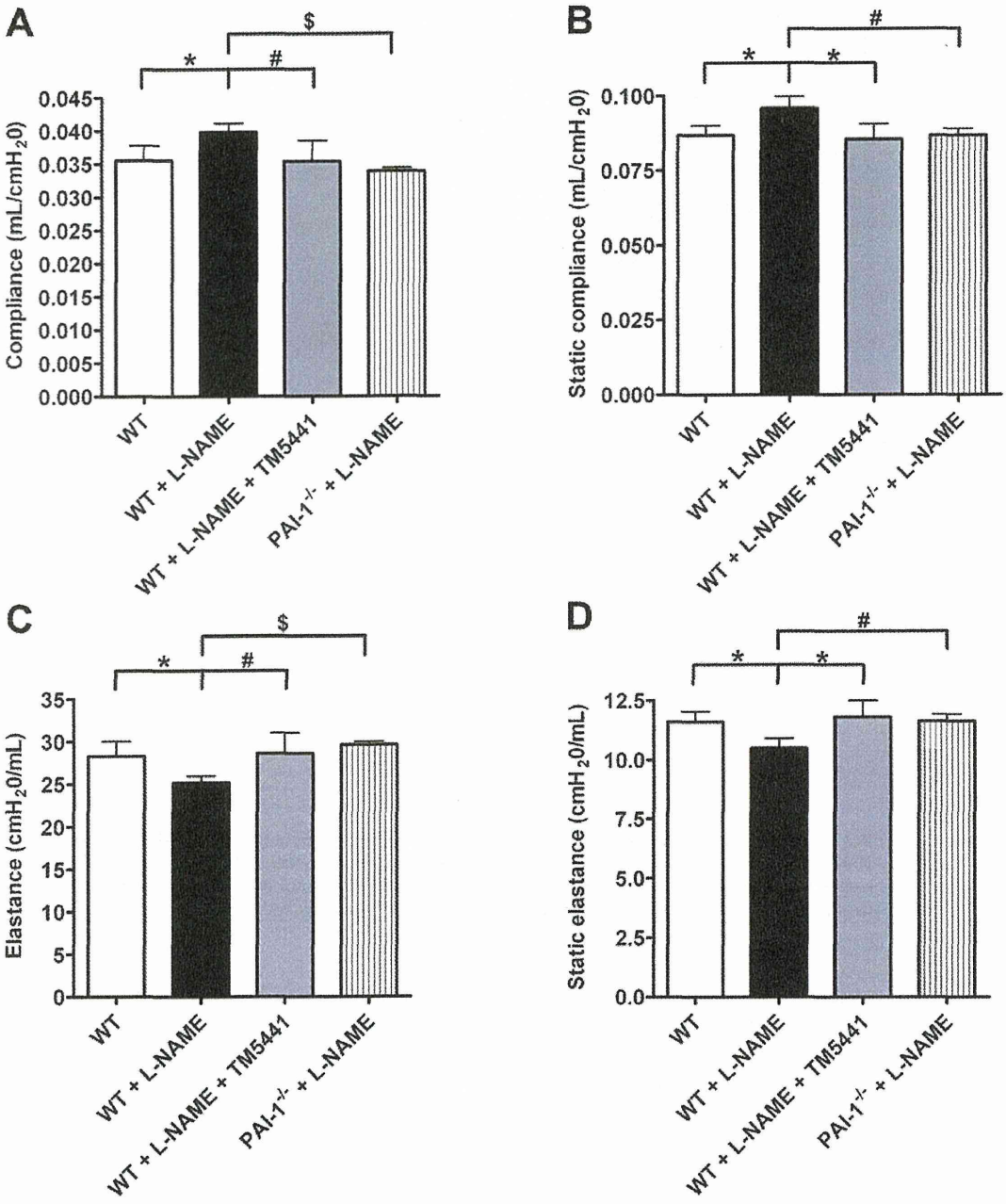

Fig 2. Effects of L-NAME on lung functional dynamics. Measurements for **(A)** compliance, **(B)** static compliance, **(C)** elastance, and **(D)** static elastance demonstrate that L-NAME-treated lungs have the functional characteristics of emphysema. Both genetic and pharmacologic inhibition of PAI-1 protected mice from lung dysfunction. **(A)** and **(C)** *P = 0.002, #P = 0.02, $P = $6.3x10^{-6}$. **(B)** and **(D)** *P = 0.004, #P = 0.01. Data are mean ± SD. n = 6–7.

doi:10.1371/journal.pone.0116504.g002

indicate that inhibition of iNOS, either pharmacologically or through genetic knockout, protects against the development of emphysema [9,10]. Additionally, a single study found that in a cigarette smoke (CS)-induced model, both L-arginine and L-NAME were somewhat protective against the development of emphysema [11].

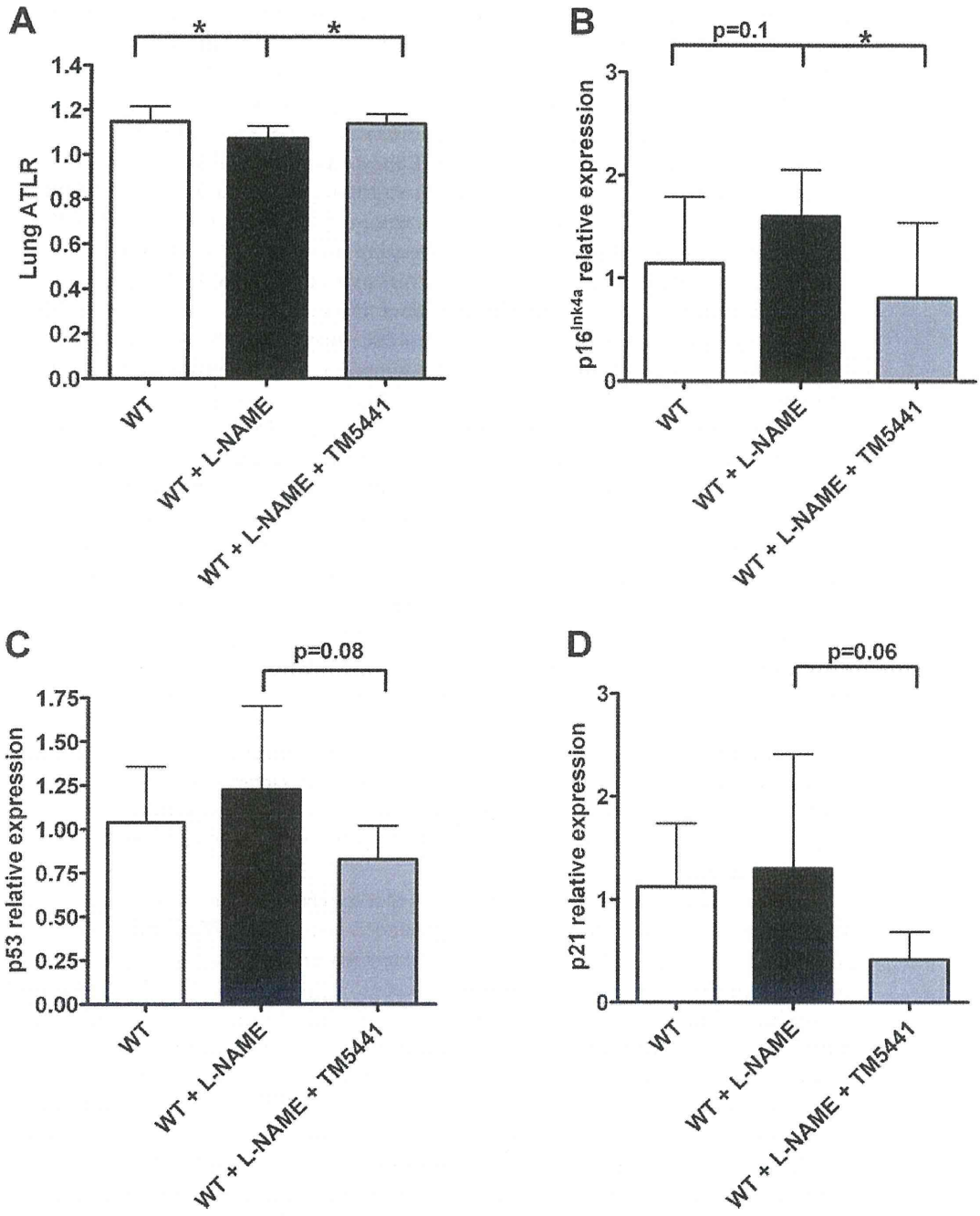

Fig 3. L-NAME-induced senescence in lung tissue. (A) ATLR measurements from 8 week-treated lungs. **(B-D)** qRT-PCR data from 1 week-treated lungs evaluating the senescence markers **(B)** $p16^{Ink4a}$, **(C)** p53, and **(D)** p21. **(A)** *P = 0.007. n = 12. **(B-D)** *P = 0.02. n = 7–11. Data are mean ± SD.

doi:10.1371/journal.pone.0116504.g003

In general, the existing literature seems to contradict our findings, as the reduction of NO production is associated with protection against emphysema. However, these results can be explained by examining the differences in the respective models used. In each of these previous studies, the authors used another stimulus (CS, elastase) to trigger emphysema initially before

investigating the isolated and selective effects of NO. Cigarette smoke and elastase both trigger an inflammatory response that is associated with intense augmentation of iNOS expression. When stimulated, iNOS produces a large amount of NO. Furthermore, iNOS activation usually occurs in an oxidative environment, which allows for NO to react with superoxide to form peroxynitrite. Normally, this functions as part of the immune response and aids in the destruction of bacterial or tumor cells. However, in both the CS and elastase models of emphysema, excess NO production from iNOS led to further tissue destruction through oxidative stress, which was associated with increased levels of peroxynitrite-induced apoptosis and reduced proliferation of alveolar epithelial cells, a key step in the development of emphysema [10]. This likely explains why previous reports found that iNOS inhibition was protective against emphysema in the CS and elastase models. Since L-NAME inhibits all three forms of NOS, the previous finding that L-NAME is protective against emphysema is likely due a reduction in iNOS-derived NO.

The administration of L-NAME alone does not appear to cause an inflammatory response, and therefore in this model iNOS is likely not activated. Instead, emphysema in this model appears to be the result of vascular senescence triggered by a lack of NO production from eNOS [12]. While generating emphysema by chronic L-NAME administration is a novel approach, other studies have demonstrated a pivotal role of endothelial cell function in lung disease. Both angiogenesis and vascular remodeling (two processes which rely on NO production) have been hypothesized to play critical roles in emphysema [13]. In guinea pigs, CS leads to reduced lung expression of eNOS and endothelial dysfunction of the pulmonary arteries, both of which preceded the development of emphysema [14]. Interestingly, in this same CS guinea pig model, co-treatment with a statin increased NO production and protected against emphysema [15]. Furthermore, eNOS has been shown to be important for compensatory lung growth. Both eNOS knockout mice and L-NAME-treated animals have impaired growth in a pneumonectomy model due to a lack of alveolar cell proliferation and reduced angiogenesis [16]. Alveolar repair in elastase-treated rats was also found to be positively correlated with eNOS expression by vascular regeneration [17]. Finally, vascular endothelial growth factor (VEGF), a known inducer of NO production, has also been implicated in the pathogenesis of emphysema [18]. Both lung-specific VEGF knockout mice [19] and mice treated with a VEGF receptor inhibitor [20] developed emphysema.

In humans, smokers have been shown to have reduced eNOS expression in their pulmonary arteries compared to non-smokers [21], along with decreases in both VEGF and VEGFR expression [22]. Smokers with emphysema had shorter telomeres and increased expression of p16 in both endothelial cells and alveolar type II cells [23]. Additionally, NO plays a major role in oxygen sensing, delivery, and utilization through SNO-based signaling. SNO-modified proteins affect the respiratory cycle, pulmonary gas exchange, and ventilation [4].

Our data expands upon this previous work, but is the first to directly look at the role of L-NAME in emphysema. We examined telomere length and $p16^{Ink4a}$ levels in the lung tissue to determine if the emphysematic pathology was a consequence of L-NAME-induced senescence. This hypothesis was confirmed, as L-NAME treatment resulted in significantly shorter telomeres after 8 weeks and an increase in $p16^{Ink4a}$ expression after just one week. Genetic deficiency and pharmacological inhibition of PAI-1 protected against the development of L-NAME-induced emphysema, as shown by both functional and histological assessments of the lungs. Furthermore, PAI-1 antagonism both preserved lung telomere length and attenuated the increases in $p16^{Ink4a}$, p53, and p21 expression. These results further support the idea that PAI-1 is a critical determinant of vascular senescence, and that L-NAME-induced emphysema is one of several pathological consequences of this senescence. Interestingly, previous work has shown that PAI-1 is upregulated in the sputum and macrophages of patients with chronic obstructive pulmonary disorder (COPD), and that it could play a pro-inflammatory role in the

pathogenesis of emphysema [24,25]. Furthermore, this increase in expression was due to oxidative stress [26]. Thus, in addition to its pro-senescent role, elevated PAI-1 may contribute to emphysema through other molecular pathways. This would further explain the protection against tissue destruction seen with genetic deficiency or TM5441-mediated inhibition of PAI-1.

While more work is needed to define fully the mechanism behind L-NAME-induced emphysema, the present findings demonstrate that the interplay between NO, PAI-1, and vascular senescence has an important impact on alveolar tissue integrity. L-NAME treatment represents a novel model for emphysema pathogenesis that could be useful in future studies.

Acknowledgments

The authors would like to thank Marissa Michaels, Aaron Place, Varun Nagpal, and Rahul Rai for their many helpful discussions regarding the work presented here.

Author Contributions

Conceived and designed the experiments: AEB ME GRSB GMM DEV. Performed the experiments: AEB ME LMN SBM GRSB GMM. Analyzed the data: AEB ME LMN GRSB GMM DEV. Contributed reagents/materials/analysis tools: GRSB GMM TM DEV. Wrote the paper: AEB ME SBM DEV.

References

1. Kaikita K, Fogo AB, Ma L, Schoenhard JA, Brown NJ, et al. (2001) Plasminogen activator inhibitor-1 deficiency prevents hypertension and vascular fibrosis in response to long-term nitric oxide synthase inhibition. Circulation 104: 839–844. PMID: 11502712
2. Kaikita K, Schoenhard JA, Painter CA, Ripley RT, Brown NJ, et al. (2002) Potential roles of plasminogen activator system in coronary vascular remodeling induced by long-term nitric oxide synthase inhibition. Journal of Molecular and Cellular Cardiology 34: 617–627. PMID: 12054849
3. Boe AE, Eren M, Murphy SB, Kamide CE, Ichimura A, et al. (2013) The PAI-1 Antagonist TM5441 Attenuates L-NAME-Induced Hypertension and Vascular Senescence. Circulation.
4. Haldar SM, Stamler JS (2013) S-nitrosylation: integrator of cardiovascular performance and oxygen delivery. Journal of Clinical Investigation 123: 101–110. doi: 10.1172/JCI62854 PMID: 23281416
5. Cawthon RM (2002) Telomere measurement by quantitative PCR. Nucleic Acids Res 30: e47. PMID: 12000852
6. Callicott RJ, Womack JE (2006) Real-time PCR assay for measurement of mouse telomeres. Comp Med 56: 17–22. PMID: 16521855
7. Vanoirbeek JA, Rinaldi M, De Vooght V, Haenen S, Bobic S, et al. (2010) Noninvasive and invasive pulmonary function in mouse models of obstructive and restrictive respiratory diseases. American Journal of Respiratory Cell and Molecular Biology 42: 96–104. doi: 10.1165/rcmb.2008-0487OC PMID: 19346316
8. Materials and methods are available as supporting material on *Science* online.
9. Lanzetti M, da Costa CA, Nesi RT, Barroso MV, Martins V, et al. (2012) Oxidative stress and nitrosative stress are involved in different stages of proteolytic pulmonary emphysema. Free Radical Biology and Medicine 53: 1993–2001. doi: 10.1016/j.freeradbiomed.2012.09.015 PMID: 23000243
10. Seimetz M, Parajuli N, Pichl A, Veit F, Kwapiszewska G, et al. (2011) Inducible NOS inhibition reverses tobacco-smoke-induced emphysema and pulmonary hypertension in mice. Cell 147: 293–305. doi: 10.1016/j.cell.2011.08.035 PMID: 22000010
11. Valenca SS, Rueff-Barroso CR, Pimenta WA, Melo AC, Nesi RT, et al. (2011) L-NAME and L-arginine differentially ameliorate cigarette smoke-induced emphysema in mice. Pulmonary Pharmacology and Therapeutics 24: 587–594. doi: 10.1016/j.pupt.2011.05.006 PMID: 21624489
12. Boe AE, Eren M, Murphy SB, Kamide CE, Ichimura A, et al. (2013) Plasminogen activator inhibitor-1 antagonist TM5441 attenuates Nomega-nitro-L-arginine methyl ester-induced hypertension and vascular senescence. Circulation 128: 2318–2324. doi: 10.1161/CIRCULATIONAHA.113.003192 PMID: 24092817

13. Siafakas NM, Antoniou KM, Tzortzaki EG (2007) Role of angiogenesis and vascular remodeling in chronic obstructive pulmonary disease. Int J Chron Obstruct Pulmon Dis 2: 453–462. PMID: 18268919

14. Ferrer E, Peinado VI, Diez M, Carrasco JL, Musri MM, et al. (2009) Effects of cigarette smoke on endothelial function of pulmonary arteries in the guinea pig. Respir Res 10: 76. doi: 10.1186/1465-9921-10-76 PMID: 19682386

15. Wright JL, Zhou S, Preobrazhenska O, Marshall C, Sin DD, et al. (2011) Statin reverses smoke-induced pulmonary hypertension and prevents emphysema but not airway remodeling. American Journal of Respiratory and Critical Care Medicine 183: 50–58. doi: 10.1164/rccm.201003-0399OC PMID: 20709821

16. Leuwerke SM, Kaza AK, Tribble CG, Kron IL, Laubach VE (2002) Inhibition of compensatory lung growth in endothelial nitric oxide synthase-deficient mice. Am J Physiol Lung Cell Mol Physiol 282: L1272–1278. PMID: 12003783

17. Ito H, Matsushita S, Ishikawa S, Goto Y, Sakai M, et al. (2013) Significant correlation between endothelial nitric oxide synthase (eNOS) expression and alveolar repair in elastase-induced rat pulmonary emphysema. Surgery Today 43: 293–299. doi: 10.1007/s00595-012-0293-7 PMID: 22911252

18. Taraseviciene-Stewart L, Voelkel NF (2008) Molecular pathogenesis of emphysema. Journal of Clinical Investigation 118: 394–402. doi: 10.1172/JCI31811 PMID: 18246188

19. Tang K, Rossiter HB, Wagner PD, Breen EC (2004) Lung-targeted VEGF inactivation leads to an emphysema phenotype in mice. J Appl Physiol (1985) 97: 1559–1566; discussion 1549. PMID: 15208295

20. Kasahara Y, Tuder RM, Taraseviciene-Stewart L, Le Cras TD, Abman S, et al. (2000) Inhibition of VEGF receptors causes lung cell apoptosis and emphysema. Journal of Clinical Investigation 106: 1311–1319. PMID: 11104784

21. Barbera JA, Peinado VI, Santos S, Ramirez J, Roca J, et al. (2001) Reduced expression of endothelial nitric oxide synthase in pulmonary arteries of smokers. American Journal of Respiratory and Critical Care Medicine 164: 709–713. PMID: 11520741

22. Kasahara Y, Tuder RM, Cool CD, Lynch DA, Flores SC, et al. (2001) Endothelial cell death and decreased expression of vascular endothelial growth factor and vascular endothelial growth factor receptor 2 in emphysema. American Journal of Respiratory and Critical Care Medicine 163: 737–744. PMID: 11254533

23. Tsuji T, Aoshiba K, Nagai A (2006) Alveolar cell senescence in patients with pulmonary emphysema. American Journal of Respiratory and Critical Care Medicine 174: 886–893. PMID: 16888288

24. Xu X, Wang H, Wang Z, Xiao W (2009) Plasminogen activator inhibitor-1 promotes inflammatory process induced by cigarette smoke extraction or lipopolysaccharides in alveolar epithelial cells. Experimental Lung Research 35: 795–805. doi: 10.3109/01902140902912519 PMID: 19916862

25. Zhang Y, Xiao W, Jiang Y, Wang H, Xu X, et al. (2012) Levels of components of the urokinase-type plasminogen activator system are related to chronic obstructive pulmonary disease parenchymal destruction and airway remodelling. Journal of International Medical Research 40: 976–985. PMID: 22906270

26. To M, Takagi D, Akashi K, Kano I, Haruki K, et al. (2013) Sputum plasminogen activator inhibitor-1 elevation by oxidative stress-dependent nuclear factor-kappaB activation in COPD. Chest 144: 515–521. doi: 10.1378/chest.12-2381 PMID: 23558707

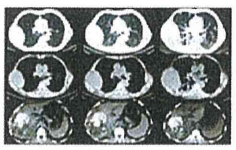

Cancer Biology & Therapy
Publication details, including instructions for authors and subscription information:
http://www.tandfonline.com/loi/kcbt20

Inhibition of plasminogen activator inhibitor-1 is a potential therapeutic strategy in ovarian cancer

Satsuki Mashiko[a], Kazuyuki Kitatani[ab], Masafumi Toyoshima[a], Atsuhiko Ichimura[c], Takashi Dan[c], Toshinori Usui[ab], Masumi Ishibashi[a], Shogo Shigeta[d], Satoru Nagase[a], Toshio Miyata[c] & Nobuo Yaegashi[a]

[a] Department of Obstetrics and Gynecology; Tohoku University Graduate School of Medicine; Sendai, Japan

[b] Tohoku Medical Megabank Organization; Tohoku University; Sendai, Japan

[c] Division of Molecular Medicine and Therapy, United Centers for Advanced Research and Translational Medicine, Tohoku University Graduate School of Medicine, Sendai, Japan

[d] Department of Obstetrics and Gynecology; Yamagata University Faculty of Medicine; Yamagata, Japan

Accepted author version posted online: 14 Jan 2015.

To cite this article: Satsuki Mashiko, Kazuyuki Kitatani, Masafumi Toyoshima, Atsuhiko Ichimura, Takashi Dan, Toshinori Usui, Masumi Ishibashi, Shogo Shigeta, Satoru Nagase, Toshio Miyata & Nobuo Yaegashi (2015) Inhibition of plasminogen activator inhibitor-1 is a potential therapeutic strategy in ovarian cancer, Cancer Biology & Therapy, 16:2, 253-260

To link to this article: http://dx.doi.org/10.1080/15384047.2014.1001271

RESEARCH PAPER

Cancer Biology & Therapy 16:2, 253–260; February 2015; © 2015 Taylor & Francis Group, LLC

Inhibition of plasminogen activator inhibitor-1 is a potential therapeutic strategy in ovarian cancer

Satsuki Mashiko[1], Kazuyuki Kitatani[1,2,*], Masafumi Toyoshima[1,*], Atsuhiko Ichimura[3], Takashi Dan[3], Toshinori Usui[1,2], Masumi Ishibashi[1], Shogo Shigeta[4], Satoru Nagase[1], Toshio Miyata[3], and Nobuo Yaegashi[1]

[1]Department of Obstetrics and Gynecology; Tohoku University Graduate School of Medicine; Sendai, Japan; [2]Tohoku Medical Megabank Organization; Tohoku University; Sendai, Japan; [3]Division of Molecular Medicine and Therapy; United Centers for Advanced Research and Translational Medicine; Tohoku University Graduate School of Medicine; Sendai, Japan; [4]Department of Obstetrics and Gynecology; Yamagata University Faculty of Medicine; Yamagata, Japan

Keywords: cancer therapeutics, clear cell carcinoma of the ovary, ovarian cancer, plasminogen activator inhibitor-1, plasminogen activator inhibitor-1 inhibitor, TM5275

Abbreviations: PAI-1, plasminogen activator inhibitor-1; PARP, poly (ADP-ribose) polymerase; PI, propidium iodide; siRNA, small interfering RNA; uPA, urokinase-type plasminogen activator.

Plasminogen activator inhibitor (PAI)-1 is predictive of poor outcome in several types of cancer. The present study investigated the biological role for PAI-1 in ovarian cancer and potential of targeted pharmacotherapeutics. In patients with ovarian cancer, PAI-1 mRNA expression in tumor tissues was positively correlated with poor prognosis. To determine the role of PAI-1 in cell proliferation in ovarian cancer, the effects of PAI-1 inhibition were examined in PAI-1-expressing ovarian cancer cells. PAI-1 knockdown by small interfering RNA resulted in significant suppression of cell growth accompanied with G2/M cell cycle arrest and intrinsic apoptosis. Similarly, treatment with the small molecule PAI-1 inhibitor TM5275 effectively blocked cell proliferation of ovarian cancer cells that highly express PAI-1. Together these results suggest that PAI-1 promotes cell growth in ovarian cancer. Interestingly, expression of PAI-1 was increased in ovarian clear cell carcinoma compared with that in serous tumors. Our results suggest that PAI-1 inhibition promotes cell cycle arrest and apoptosis in ovarian cancer and that PAI-1 inhibitors potentially represent a novel class of anti-tumor agents.

Introduction

Ovarian cancer is the most lethal gynecologic malignancy.[1] Despite advances in debulking surgery combined with platinum- and taxane-based chemotherapies, the overall cure rate has not improved appreciably. Hence, there is a need to develop new therapeutic strategies for this malignancy.

Plasminogen activator inhibitor-1 (PAI-1), also known as SERPINE1, is a serine protease inhibitor that functions as a plasma inhibitor of urokinase-type plasminogen activator (u-PA), thus regulating fibrinolytic systems as well as tissue remodeling.[2,3] The PAI-1 and u-PA axis is one of the most investigated protease systems in cancer. Many studies have demonstrated that high levels of PAI-1 are predictive of a poor clinical outcome in many types of cancer, including gastric,[4] colorectal,[5] breast,[6-8] lung,[9] renal[10] and ovarian cancer,[11-13] suggesting possible involvement of PAI-1 in cancer progression.

PAI-1 is a multi-functional protein that plays an important role in regulating cell proliferation, adhesion, migration, and signal transduction.[14] Recent studies have also demonstrated a role for PAI-1 in cancer cell biology. PAI-1 was shown to contribute to cell proliferation by altering response to uPA in MCF-7 cells.[15] PAI-1 not only has anti-apoptotic effects in lung, breast and colon cancer cell lines, but may also be a possible therapeutic target for cancer treatment.[16] However, understanding the functions of PAI-1 in ovarian cancer still remains largely elusive.

In the present study, we investigated a role for PAI-1 in cell proliferation and the potential of PAI-1 as a possible therapeutic target in ovarian cancer. Moreover, PAI-1 expression in histological subtypes of ovarian cancer was also evaluated. We also discuss the potential of a small molecule PAI-1 inhibitor TM5275[17,18] as an anti-cancer drug for ovarian malignancy.

Results

Upregulation of PAI-1 as a prognostic marker in ovarian cancer

To test the biological significance of PAI-1 (SERPINE1) in ovarian cancer, we first analyzed its expression pattern using a public access database of patients with ovarian cancer, as described in a previous population-based study.[19] Using 2 independent microarray probe sets that were found to represent consistent PAI-1 expression, results demonstrated that the group

*Correspondence to: Kazuyuki Kitatani; Email: kitatani@med.tohoku.ac.jp; or Masafumi Toyoshima; Email: m-toyo@med.tohoku.ac.jp
Submitted: 06/04/2014; Revised: 10/14/2014; Accepted: 12/18/2014
http://dx.doi.org/10.1080/15384047.2014.1001271